TU Delft

Delft University of Technology

Tuning the Q -factor of nanomechanical string resonators by torsion support design

Li, Zichao; Xu, Minxing; Norte, Richard A.; Aragón, Alejandro M.; Van Keulen, Fred; Alijani, Farbod; Steeneken, Peter G.

DOI
10.1063/5.0133177

Publication date
2023

Document Version
Final published version

Published in
Applied Physics Letters

Citation (APA)
Li, Z., Xu, M., Norte, R. A., Aragón, A. M., Van Keulen, F., Alijani, F., & Steeneken, P. G. (2023). Tuning the Q -factor of nanomechanical string resonators by torsion support design. *Applied Physics Letters*, *122*(1), Article 013501. https://doi.org/10.1063/5.0133177

Important note
To cite this publication, please use the final published version (if applicable).
Please check the document version above.

Copyright
Other than for strictly personal use, it is not permitted to download, forward or distribute the text or part of it, without the consent of the author(s) and/or copyright holder(s), unless the work is under an open content license such as Creative Commons.

Takedown policy
Please contact us and provide details if you believe this document breaches copyrights.
We will remove access to the work immediately and investigate your claim.

This work is downloaded from Delft University of Technology.
For technical reasons the number of authors shown on this cover page is limited to a maximum of 10.

Applied Physics Letters

Tuning the Q-factor of nanomechanical string resonators by torsion support design

Cite as: Appl. Phys. Lett. **122**, 013501 (2023); https://doi.org/10.1063/5.0133177
Submitted: 02 November 2022 • Accepted: 15 December 2022 • Published Online: 03 January 2023

Zichao Li, Minxing Xu, Richard A. Norte, et al.

View Online Export Citation CrossMark

ARTICLES YOU MAY BE INTERESTED IN

Readout of a quantum processor with high dynamic range Josephson parametric amplifiers
Applied Physics Letters **122**, 014001 (2023); https://doi.org/10.1063/5.0127375

Generation of 2D and 3D acoustic lattices in midair using polygonal active diffraction gratings
Applied Physics Letters **122**, 012201 (2023); https://doi.org/10.1063/5.0126728

Layered, tunable graphene oxide-nylon composite heterostructures for wearable electrocardiogram sensors
Applied Physics Letters **122**, 013701 (2023); https://doi.org/10.1063/5.0120774

AIP Publishing

© 2023 Author(s).

Applied Physics Letters ARTICLE scitation.org/journal/apl

Tuning the Q-factor of nanomechanical string resonators by torsion support design

Cite as: Appl. Phys. Lett. **122**, 013501 (2023); doi: 10.1063/5.0133177
Submitted: 2 November 2022 · Accepted: 15 December 2022 ·
Published Online: 3 January 2023

View Online Export Citation CrossMark

Zichao Li,[1,a)] Minxing Xu,[1,2] Richard A. Norte,[1,2] Alejandro M. Aragón,[1] Fred van Keulen,[1] Farbod Alijani,[1] and Peter G. Steeneken[1,2,a)]

AFFILIATIONS

[1]Department of Precision and Microsystems Engineering, Delft University of Technology, Mekelweg 2, 2628 CD Delft, The Netherlands
[2]Kavli Institute of Nanoscience, Delft University of Technology, Lorentzweg 1, 2628 CJ Delft, The Netherlands

[a)]**Authors to whom correspondence should be addressed:** z.li-16@tudelft.nl and p.g.steeneken@tudelft.nl

ABSTRACT

In recent years, the *Q*-factor of Si_3N_4 nanomechanical resonators has significantly been increased by soft-clamping techniques using large and complex support structures. To date, however, obtaining similar performance with smaller supports has remained a challenge. Here, we make use of torsion beam supports to tune the *Q*-factor of Si_3N_4 string resonators. By design optimization of the supports, we obtain a 50% *Q*-factor enhancement compared to the standard clamped–clamped string resonators. By performing experimental and numerical studies, we show that further improvement of the *Q*-factor is limited by a trade-off between maximizing stress and minimizing torsional support stiffness. Thus, our study also provides insight into dissipation limits of high-stress string resonators and outlines how advanced designs can be realized for reaching ultimate $f_0 \times Q$ product while maintaining a small footprint.

© 2023 Author(s). All article content, except where otherwise noted, is licensed under a Creative Commons Attribution (CC BY) license (http://creativecommons.org/licenses/by/4.0/). https://doi.org/10.1063/5.0133177

Nanomechanical resonators are receiving growing interest owing to their high force sensitivity and ultra-low dissipation. They have demonstrated strong potential for mass sensing,[1,2] force sensing,[3–6] and transducer applications.[7–9] Moreover, nanomechanical systems are promising platforms to explore fundamental physics in both the classical[10] and quantum[11–14] regimes. In recent decades, there has been a tremendous drive toward increasing the mechanical *Q*-factor of nanomechanical resonators to maximally benefit from the important performance advantages this offers:[15–17] when dissipation is low, resonant sensors, clocks, and frequency synthesizers can be operated at large oscillation amplitudes with low power. Moreover, low losses diminish the thermomechanical-noise induced motion of the resonator via the fluctuation–dissipation theorem.[15,18] This low noise results in higher signal-to-noise ratio and improves the limit of detection in sensor applications. Finally, in the quantum regime, a high-*Q* isolates the resonant mode from being affected by thermomechanical noise and, thus, protects quantum states from decoherence.[19,20]

A main methodology for increasing *Q* in Si_3N_4 resonators has been the increase in tension.[21–24] This dissipation-dilution mechanism has resulted in large *Q* enhancements, especially in materials like Si_3N_4 that can be grown with high intrinsic tensile stress.[25,26] However, the increase in stress in a clamped–clamped string is associated with an increase in the bending curvature near the clamping points which, in turn, limits the dissipation-dilution factor.[27,28] Recent efforts have enabled mitigating these losses by soft-clamping techniques, which involve large support structures that allow high-stress to be preserved while maintaining small curvatures near the edge of the resonant mode.[17,29,30]

Here, we investigate an alternative approach for reducing dissipation in Si_3N_4 string resonators by suspending the string using torsion beam supports instead of the more conventional direct clamping at the edges.[31,32] To determine the *Q*-factor limits of this approach, we study experimentally, analytically, and numerically—by means of the Finite Element Method (FEM)—how the support dimensions can be used to optimize the resonance frequency and *Q*-factor in string resonators. We show that the supports enable stress engineering over a wide range from 0.10 to 0.80 GPa, while also controlling the torsional and out-of-plane translational stiffness of supports. We also demonstrate a *Q* enhancement of 50%, which is limited due to a support design trade-off between maximizing the string's stress and minimizing the supports' torsional stiffness.

© Author(s) 2023

To get an intuitive understanding of this trade-off, before discussing detailed analytical and numerical models (see also Secs. S3–S5 of the supplementary material), we first analyze a simplified analytical model of the Q-factor of string resonators with non-ideal supports. Theoretically, an ideal string resonator would be free to rotate around its pinned endpoints. In practice, however, as we show in Fig. 1, the supports always have a finite torsional stiffness k_t and out-of-plane translational stiffness k that will cause the support point to move and rotate along with the resonant motion of the string. Although this support motion has little effect on the resonance frequency and mode shape of the string, it can have a significant influence on the dissipation in nanomechanical string resonators.[10,33,34] To estimate the effect of supports on the mechanical Q, we consider the string resonator with a known tension F_b and assume that the tension is high enough to neglect the effects of the support on the mode shape, such that the fundamental resonant mode can be assumed as $\phi_b(x) = \phi_0 \sin(\pi x/L_b)$, where x denotes spatial coordinate, ϕ_0 is the amplitude of the mode shape, and L_b is the resonator's length. As a consequence of its motion, the string will exert a force and torque on the support with energy storage $W_k = \frac{1}{2}k\Delta_o^2$ and $W_t = \frac{1}{2}k_t\theta^2$, for small angles $\theta \approx \frac{d\phi_b(x)}{dx}|_{x=0}$, associated with the supports' out-of-plane deflection Δ_o and torsional rotation θ, respectively. We also note that the force balance in the out-of-plane z-direction is given by $F_{b,z} = F_b \frac{d\phi_b(x)}{dx}|_{x=0} = k\Delta_o$, where $F_b = A_b\sigma_b$ and A_b is the cross-sectional area of the string. Using the given mode shape, the strain energy stored in the fundamental mode of the string can be written as $W_\sigma = \pi^2 F_b \phi_0^2/(4L_b)$.

After having established these equations, we obtain Q of a string resonator[33] with translational and torsional supports,

$$Q = \left(\frac{W_\sigma}{2W_k + 2W_t} + 1\right) Q_0 \approx \frac{Q_0 L_b}{4}\left(\frac{F_b}{k} + \frac{k_t}{F_b}\right)^{-1}, \quad (1)$$

where Q_0 is the intrinsic quality factor due to material damping. The equation shows that, as long as $F_b/k \ll k_t/F_b$, an increase in tension F_b can enlarge the Q-factor of the string resonator via dissipation dilution. The increase in Q continues until around $F_b/k \approx k_t/F_b$ and at $F_{b,max} = \sqrt{k_t k}$ the Q-factor will show a maximum value $Q_{max} = \frac{Q_0 L_b}{8}\sqrt{k/k_t}$.

This approximate equation tells us that optimization of support structures requires to maximize their out-of-plane translational stiffness k, while minimizing their torsional stiffness k_t, in order to minimize losses due to bending and torsional motion. Furthermore, a third important requirement is that in-plane stiffness k_i of the support [see Figs. 1 and Sec. S3(a) of the supplementary material] and the material's initial isotropic pre-stress σ_0 are high enough to prevent the string tension F_b from dropping far below $F_{b,max}$ after the release etch. This tension reduction is a consequence of the support's in-plane deflection $\Delta_i = F_b/k_i$. To validate these guidelines and explore their potential for enhancing Q, we will now present a more accurate experimental and numerical study of the effect of the support design on the Q-factor of string resonators.

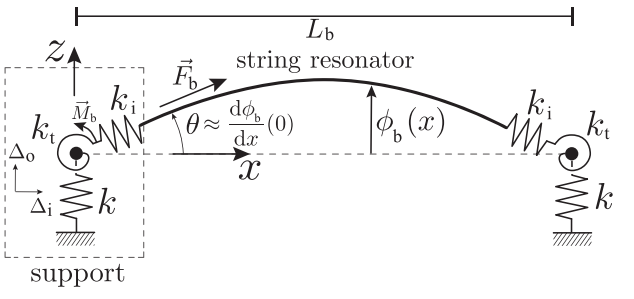

FIG. 1. Schematic model for a string resonator with non-ideal supports. At the clamping points, the string exerts a tension $\vec{F}_b$ and a torque $\vec{M}_b$ on the support, which are balanced by the in-plane translational spring k_i, the out-of-plane translational spring k, and the torsional spring k_t of the support structure.

The string resonators in this work are fabricated from a high-stress Si_3N_4 layer with a thickness $h = 340$ nm and an initial pre-stress $\sigma_0 = 1.1$ GPa grown by low pressure chemical vapor deposition (LPCVD) on a silicon substrate.[35] The devices are suspended by a fluorine-based (SF_6) deep reactive ion underetching step. All nanomechanical resonators studied in this work are fabricated on the same chip, which has the advantage of providing identical pre-stress σ_0 and thickness h of the Si_3N_4 layer.

To optimize the support design, control is needed over the torsional stiffness k_t, out-of-plane translational stiffness k, and string stress σ_b. For this purpose, we utilize a rectangular doubly clamped support structure with length L_s and width w_s. The resonator is connected at both ends to the center of such a torsion beam support. The studied Si_3N_4 strings have lengths $L_b = 100$, 200, 300, and 400 μm. The support length is always kept at $L_s = 31$ μm while the support width varies from $w_s = 1$ μm to 8 μm.

Figure 2(a) shows a picture of an actual device, whose fundamental resonance frequency is characterized using the measurement setup shown in Fig. 2(b). The chip with string resonators is placed on a piezo actuator that shakes the chip to drive the resonators into resonance. To characterize the resonance frequencies and Q-factors, we use an MSA400 Polytec Laser Doppler Vibrometer connected to a Zurich Instruments HF2LI lock-in amplifier to measure the out-of-plane velocity of the middle of the string, as shown in Fig. 2(b). The measurements are performed at room temperature in a vacuum chamber at a pressure below 2×10^{-6} mbar to minimize the effect of gas damping.

For each resonator, we perform a frequency sweep in the linear regime to determine the resonance frequency f_0 of the fundamental out-of-plane mode by fitting a Lorentzian to the data points [see Fig. 2(c)]. To ensure that the demodulator filter bandwidth does not affect the determination of the Q-factor, we determine Q from the ring-down measurements [see Fig. 2(d)]. Thus, the measured resonance frequencies f_0 and Q-factors of 24 clamped–clamped string resonators with varying values of L_b and w_s are tabulated in S1 of the supplementary material. Resonance frequencies range from 0. 26 to 2.40 MHz. In addition, we assume that Si_3N_4 is isotropic, with Young's modulus E_1 and loss modulus E_2 identical in all directions, and characterize a set of singly clamped Si_3N_4 cantilevers to precisely determine the Young's modulus $E_1 = 271$ GPa, and the intrinsic quality factor $Q_0 = 11\,774$ due to material losses, which is close to literature values[25,35] (see S2 of the supplementary material).

A key advantage of the torsion beam support design is that it provides an effective way to control the stress σ_b in the string resonators made from a strained layer with an initial stress σ_0. It, thus, provides an alternative to the recently presented geometric stress tuning

© Author(s) 2023

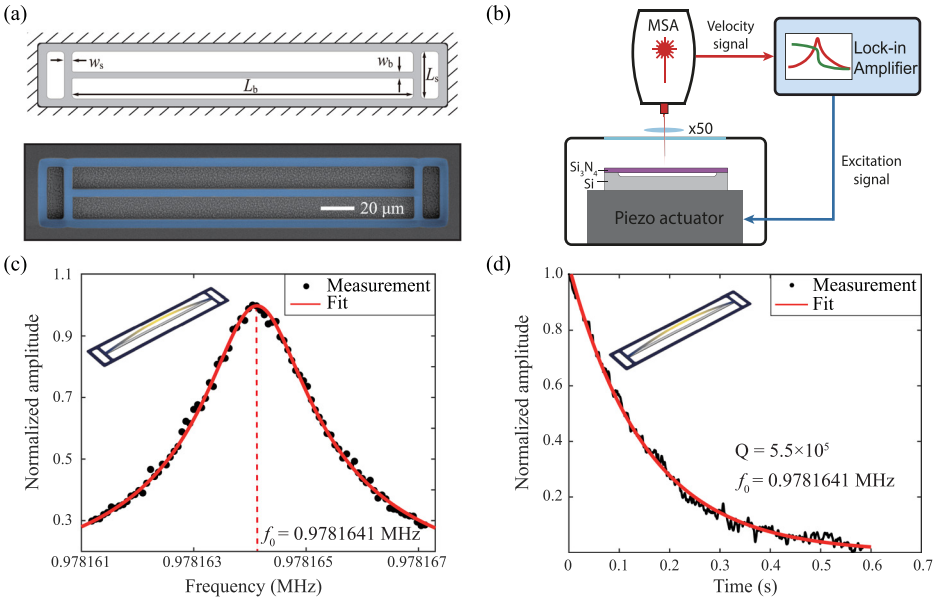

FIG. 2. Experimental characterization of the nanomechanical resonators. (a) False-colored scanning electron microscope (SEM) image of an string resonator with $L_b = 200$, $w_b = 4$, $L_s = 31$, $w_s = 4.5\,\mu$m, and the corresponding numerical model. (b) Schematics of measurement setup. (c) Harmonic response of the string resonator shown in (a), excited near its fundamental resonance frequency. (d) Ring-down measurement of the string resonator in (a), after stopping the resonant driving of the fundamental mode. The *y*-axis is normalized to the amplitude at $t = 0$.

method[32] for obtaining a large number of string resonators, with widely varying σ_b, from 0.15 to 0.74 GPa [see Fig. 3(b)], on the same chip by adjusting the support geometry. After the Si release etch, the high-stress Si_3N_4 string resonators are suspended, and as a consequence of the finite in-plane stiffness k_i of the support, the string becomes slightly shorter, which causes the string stress to reduce to σ_b. In Fig. 3(a), we show FEM simulations of the effect of the support design on the string stress $\sigma_{b,FEM}$. For small values of w_s, k_i reduces, and consequently σ_b in the string is lower after the release etch.

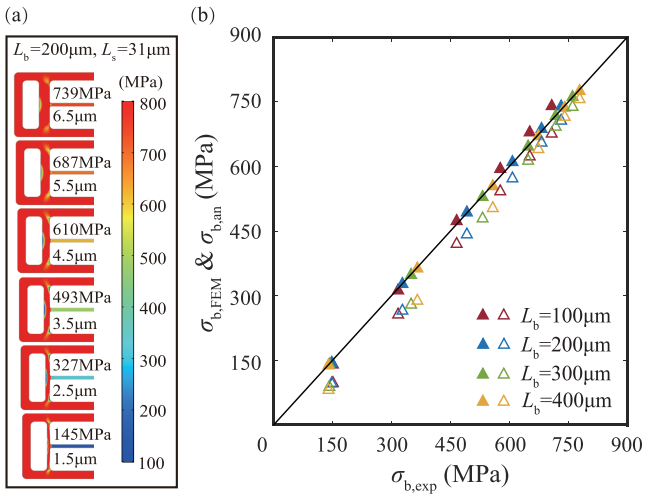

FIG. 3. Comparison between experimental and simulated stress. (a) FEM simulations show how the string's stress after the release can be varied using the support width design. (b) $\sigma_{b,FEM}$ obtained from FEM (filled triangles) and $\sigma_{b,an}$ calculated from Eq. (3) (open triangles, Poisson ratio taken as $\nu = 0.23$[28,35]) are plotted against experimentally obtained $\sigma_{b,exp}$ using Eq. (2) for resonators of different lengths.

Before analyzing the Q of the resonators, we use their measured f_0 to determine the string stress using the equation for the fundamental resonance frequency $f_0 \approx \sqrt{\sigma_{b,exp}/(4L_b^2\rho)}$ of a simply supported string,

$$\sigma_{b,exp} \approx 4\rho L_b^2 f_0^2, \tag{2}$$

where the literature value of Si_3N_4 mass density is taken as $\rho = 3100\,\mathrm{kg/m^3}$. For the high-stress devices in this work, the effect of bending rigidity on σ_b is less than 1% and is, therefore, neglected.[31] To validate this procedure, we plot in Fig. 3(b) the value of $\sigma_{b,FEM}$ (filled triangles) as obtained from FEM [Fig. 3(a)] against the experimentally determined value $\sigma_{b,exp}$ from Eq. (2) for all 24 devices. The correspondence between experiments and simulations gives us confidence in using Eq. (2) for extracting the stress in string resonators. The observed stress tuning effect can also be approximated by static analysis [see Sec. S3(a) of the supplementary material] of the string after the release etch,

$$\sigma_{b,an} \approx \frac{\sigma_0(1-\nu)}{1 + 2E_1A_b/(k_iL_b)}. \tag{3}$$

The string stress calculated from this equation is also shown as open triangles in Fig. 3(b), with the analytical equation providing quite a good approximation of $\sigma_{b,FEM}$ at high stress values, but deviating at lower stresses for the supports with small widths.

Although the resonance frequency mainly depends on the string stress σ_b, which in turn depends on the in-plane stiffness k_i of the support, the Q-factor is also sensitive to the torsional and out-of-plane translational stiffness of the support as expected from Eq. (1). In Fig. 4, we plot the experimentally measured Q-factors for various string lengths L_b and support widths w_s. Figure 4(a) shows that a large range of resonance frequencies f_0 and Q-factors can be covered by tuning these two parameters on the same chip. In Fig. 4(b), it can be seen that for each value of L_b the Q-factor increases with increasing σ_b, as

© Author(s) 2023

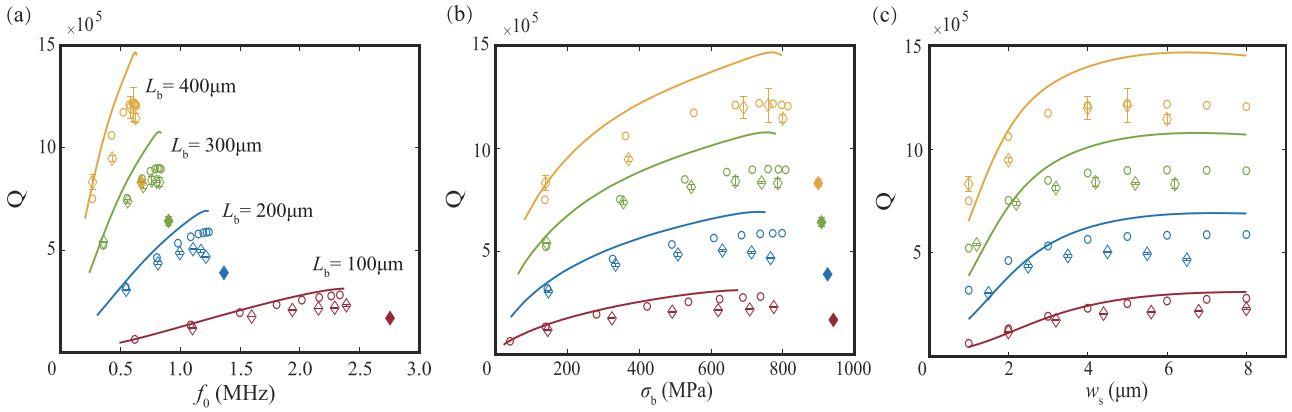

FIG. 4. Effect of support design on Q. The figures show Q as a function of fundamental resonance frequency f_0 (a), stress $\sigma_{b,exp}$ calculated from Eq. (2) (b), and support width w_s (c). Experimental results (diamonds) are compared to those obtained by FEM (circles) and analytically (solid lines). The solid diamonds represent the experimental Q-factors of directly clamped strings without torsion supports. All samples have $L_s = 31$ and $w_b = 2\,\mu$m, while L_b and w_s are varied. All data with the same L_b [labels in (a)] has the same color.

expected from dissipation dilution, with Q increasing approximately proportional to L_b [as expected from Eq. (1)]. However, around a stress of 700 MPa, the $Q - \sigma_b$ curve flattens off, showing a maximum value above which a slight reduction in Q is observed.

Although we anticipated such an optimal value of Q in Eq. (1), the actual situation is somewhat more complicated. Since in Fig. 4(b) it is not only σ_b ($F_b = A_b\sigma_b$) that is increasing but actually increasing w_s also causes simultaneous increase in the support's k_t and k. To fully capture this effect, we present in Fig. 4 simulated values of Q both using FEM (circles) and using an analytical model (solid lines) that solves the Euler–Bernoulli beam equation in the presence of stress[10] for the boundary conditions given in Fig. 1 (see Secs. S4 and S5 of the supplementary material). The FEM simulations capture the experimental Q values closely. The analytical model, which determines the values of k_t and k from the support geometry [see Sec. S3(b) of the supplementary material], also captures Q quite well, although it overestimates Q for the longer string lengths by 17%. It is important to note that the maximum values obtained in strings with torsion beam supports (open diamonds) is substantially higher (up to 50%) than the Q obtained in directly clamped strings of the same length (filled diamonds), despite the higher stress σ_b in those directly clamped ones [see Fig. 4(b)]. This observation provides evidence that not only high string stress σ_b but also low torsional stiffness of the support k_t is required for obtaining high Q.

Moreover, we should realize that to reach a high maximum quality factor $Q_{max} \approx \frac{Q_0 L_b}{8}\sqrt{k/k_t}$ requires not only a low torsional stiffness k_t but also a large out-of-plane translational stiffness k. However, for the torsion design presented here—and many other compliant support designs—decreasing k_t, e.g., by reducing w_s or increasing L_s, will also decrease k such that their ratio is not easily tuned by the orders of magnitude that are needed to reach record Q values. An extensive study of the Q-factor as a function of w_s and L_s is presented in Sec. S5 of the supplementary material to assess the influence from supports' geometry over a larger parameter range. The presented models and experiments, thus, expose a trade-off that has to be made among σ_b, k, and k_t, which limit the ultimate Q that can be obtained using string resonators with compliant supports.

A potential method to overcome this limitation is the use of periodic string resonators that move out of phase, like the one illustrated in Fig. 5. By having anti-symmetrically vibrating resonators with respect to a central support, the effect of two opposite forces F_b on the support cancels, and the support displacement is equal to zero. This allows reducing k_t to a very low value without diminishing σ_b. This periodic resonator configuration resolves two issues: first, the spring k is not deflected in the out-of-plane direction [such that W_k is zero in Eq. (1)], and second, σ_b in the string does not depend on the in-plane stiffness k_i of the support anymore, since the in-plane displacement of the support has also become zero. As a consequence, k_t can be minimized without leading to a reduction in k_i and σ_b.

However, in a linear configuration, this periodicity cannot be continued indefinitely, and non-periodic end-supports are needed. An interesting idea to avoid the necessity of such end-supports is to couple the periodic anti-symmetric resonators at a $180°/n$ (integer $n > 1$) angle via torsion springs with very low k_t in a regular polygon arrangement, as was recently demonstrated,[35,36] yielding record-high Q values exceeding a billion.

In the presence of periodic boundary conditions, k and k_i become infinitely large such that the only relevant parameters in Eq. (1) are F_b and k_t. Thus, the ultimate value of the f_0Q product (for $h^2 \ll w_s^2$ and assuming other loss mechanisms are negligible) approximately becomes (see S6 of the supplementary material),

$$(f_0 \times Q)_{max} \approx \frac{3Q_0(1-\nu)^{\frac{3}{2}}\sigma_0^{\frac{1}{2}}w_b L_s}{8\rho^{\frac{1}{2}}w_s^3}. \quad (4)$$

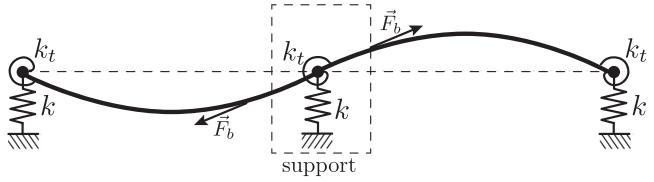

FIG. 5. Periodic string resonator configuration. The anti-symmetric vibration mode stabilizes the translational displacement of the central support and preserves the high stress in the string at the same time.

© Author(s) 2023

It is interesting to note that in the ultimate limit, the f_0Q product in Eq. (4) has become independent of the string thickness and string length, such that it mainly depends on the design of the support (w_s and L_s) and increasing it will require supports with very low torsional stiffness.

In conclusion, we have analyzed the effect of support design on the Q-factor of high-stress Si_3N_4 nanomechanical string resonators. By engineering torsion beam supports, we control the resonator's stress σ_b as well as the support's torsional stiffness k_t and out-of-plane translational stiffness k without any post-fabrication manipulation.[23] Tuning these parameters over a large range allows us to investigate their role on the dissipation and present validated models for estimating the mechanical Q of string resonators. More importantly, we find that the interplay between these geometric parameters allows us to determine the optimal support geometry that optimizes Q for string resonators of fixed length. The Q cannot be increased indefinitely due to design trade-offs that limit the possibility to design supports that both have low torsional stiffness k_t and high in-plane stiffness k_i. It is this realization that explains the success of soft-clamping and periodic clamping methodologies which can further increase Q above the limits of simple string resonators. The challenge remains to find the most effective way to create high-Q resonators with minimal device dimensions. The presented models, methods, and insight can help toward achieving higher Q-factors without requiring ever increasing device areas and provide a route toward realizing arrays of sensor devices with widely varying values of f_0 and Q on the same chip with optimal sensitivity and resolution.[37]

See the supplementary material for the measurement data and characterization of Si_3N_4 as well as the FEM simulation and detailed analytical derivation about Q-factor of string resonators with torsion supports.

This work has received fundings from ERC starting grant ENIGMA (No. 802093). Z.L. acknowledges the financial support from the China Scholarship Council. This work is also part of the project Probing the physics of exotic superconductors with microchip Casimir experiments (No. 740.018.020) of the research programme NWO Start-up which is partly financed by the Dutch Research Council (NWO). M.X. and R.N. acknowledge the valuable support from the Kavli Nanolab Delft.

AUTHOR DECLARATIONS

Conflict of Interest

The authors have no conflicts to disclose.

Author Contributions

Zichao Li: Conceptualization (lead); Data curation (equal); Formal analysis (equal); Funding acquisition (equal); Investigation (equal); Methodology (equal); Project administration (equal); Resources (equal); Software (equal); Visualization (equal); Writing – original draft (lead). **Minxing Xu:** Methodology (supporting); Resources (supporting). **Richard A. Norte:** Funding acquisition (supporting); Methodology (supporting); Resources (supporting); Writing – review & editing (supporting). **Alejandro M. Aragón:** Conceptualization (equal); Project administration (supporting); Supervision (supporting); Writing – review & editing (supporting). **Fred van Keulen:** Conceptualization (supporting); Supervision (supporting). **Farbod Alijani:** Conceptualization (lead); Formal analysis (equal); Funding acquisition (equal); Project administration (equal); Resources (equal); Supervision (lead); Writing – review & editing (equal). **Peter Steeneken:** Conceptualization (lead); Formal analysis (equal); Funding acquisition (equal); Project administration (equal); Resources (equal); Supervision (lead); Writing – review & editing (lead).

DATA AVAILABILITY

The data that support the findings of this study are available from the corresponding authors upon request.

REFERENCES

[1]A. K. Naik, M. Hanay, W. Hiebert, X. Feng, and M. L. Roukes, "Towards single-molecule nanomechanical mass spectrometry," Nat. Nanotechnol. **4**, 445–450 (2009).
[2]J. Chaste, A. Eichler, J. Moser, G. Ceballos, R. Rurali, and A. Bachtold, "A nanomechanical mass sensor with yoctogram resolution," Nat. Nanotechnol. **7**, 301–304 (2012).
[3]H. Mamin and D. Rugar, "Sub-attonewton force detection at millikelvin temperatures," Appl. Phys. Lett. **79**, 3358–3360 (2001).
[4]D. Rugar, R. Budakian, H. Mamin, and B. Chui, "Single spin detection by magnetic resonance force microscopy," Nature **430**, 329–332 (2004).
[5]M. Wang, R. Zhang, R. Ilic, V. Aksyuk, and Y. Liu, "Frequency stabilization of nanomechanical resonators using thermally invariant strain engineering," Nano Lett. **20**, 3050–3057 (2020).
[6]F. J. Giessibl and H. Bielefeldt, "Physical interpretation of frequency-modulation atomic force microscopy," Phys. Rev. B **61**, 9968 (2000).
[7]M. Suter, O. Ergeneman, J. Zürcher, S. Schmid, A. Camenzind, B. J. Nelson, and C. Hierold, "Superparamagnetic photocurable nanocomposite for the fabrication of microcantilevers," J. Micromech. Microeng. **21**, 025023 (2011).
[8]J. D. Teufel, D. Li, M. Allman, K. Cicak, A. Sirois, J. Whittaker, and R. Simmonds, "Circuit cavity electromechanics in the strong-coupling regime," Nature **471**, 204–208 (2011).
[9]T. J. Kippenberg and K. J. Vahala, "Cavity optomechanics: Back-action at the mesoscale," Science **321**, 1172–1176 (2008).
[10]S. Schmid, L. G. Villanueva, and M. L. Roukes, *Fundamentals of Nanomechanical Resonators* (Springer, 2016), Vol. 49.
[11]A. D. O'Connell, M. Hofheinz, M. Ansmann, R. C. Bialczak, M. Lenander, E. Lucero, M. Neeley, D. Sank, H. Wang, M. Weides *et al.*, "Quantum ground state and single-phonon control of a mechanical resonator," Nature **464**, 697–703 (2010).
[12]R. A. Norte, J. P. Moura, and S. Gröblacher, "Mechanical resonators for quantum optomechanics experiments at room temperature," Phys. Rev. Lett. **116**, 147202 (2016).
[13]M. Rossi, D. Mason, J. Chen, Y. Tsaturyan, and A. Schliesser, "Measurement-based quantum control of mechanical motion," Nature **563**, 53–58 (2018).
[14]T. Purdy, K. Grutter, K. Srinivasan, and J. Taylor, "Quantum correlations from a room-temperature optomechanical cavity," Science **356**, 1265–1268 (2017).
[15]J. M. L. Miller, A. Ansari, D. B. Heinz, Y. Chen, I. B. Flader, D. D. Shin, L. G. Villanueva, and T. W. Kenny, "Effective quality factor tuning mechanisms in micromechanical resonators," Appl. Phys. Rev. **5**, 041307 (2018).
[16]E. Kenig and M. Cross, "Frequency precision of oscillators based on high-Q resonators," arXiv:1510.07331 (2015).
[17]A. H. Ghadimi, D. J. Wilson, and T. J. Kippenberg, "Radiation and internal loss engineering of high-stress silicon nitride nanobeams," Nano Lett. **17**, 3501–3505 (2017).
[18]H. B. Callen and T. A. Welton, "Irreversibility and generalized noise," Phys. Rev. **83**, 34 (1951).
[19]U. Delić, M. Reisenbauer, K. Dare, D. Grass, V. Vuletić, N. Kiesel, and M. Aspelmeyer, "Cooling of a levitated nanoparticle to the motional quantum ground state," Science **367**, 892–895 (2020).

© Author(s) 2023

[20]J. Guo, R. Norte, and S. Gröblacher, "Feedback cooling of a room temperature mechanical oscillator close to its motional ground state," Phys. Rev. Lett. **123**, 223602 (2019).
[21]Q. P. Unterreithmeier, T. Faust, and J. P. Kotthaus, "Damping of nanomechanical resonators," Phys. Rev. Lett. **105**, 027205 (2010).
[22]D. R. Southworth, R. A. Barton, S. S. Verbridge, B. Ilic, A. D. Fefferman, H. G. Craighead, and J. M. Parpia, "Stress and silicon nitride: A crack in the universal dissipation of glasses," Phys. Rev. Lett. **102**, 225503 (2009).
[23]S. S. Verbridge, D. F. Shapiro, H. G. Craighead, and J. M. Parpia, "Macroscopic tuning of nanomechanics: Substrate bending for reversible control of frequency and quality factor of nanostring resonators," Nano Lett. **7**, 1728–1735 (2007).
[24]P.-L. Yu, T. Purdy, and C. Regal, "Control of material damping in high-Q membrane microresonators," Phys. Rev. Lett. **108**, 083603 (2012).
[25]L. G. Villanueva and S. Schmid, "Evidence of surface loss as ubiquitous limiting damping mechanism in SiN micro- and nanomechanical resonators," Phys. Rev. Lett. **113**, 227201 (2014).
[26]S. A. Fedorov, N. J. Engelsen, A. H. Ghadimi, M. J. Bereyhi, R. Schilling, D. J. Wilson, and T. J. Kippenberg, "Generalized dissipation dilution in strained mechanical resonators," Phys. Rev. B **99**, 054107 (2019).
[27]P. Sadeghi, M. Tanzer, S. L. Christensen, and S. Schmid, "Influence of clamp-widening on the quality factor of nanomechanical silicon nitride resonators," J. Appl. Phys. **126**, 165108 (2019).
[28]S. A. Fedorov, A. Beccari, N. J. Engelsen, and T. J. Kippenberg, "Fractal-like mechanical resonators with a soft-clamped fundamental mode," Phys. Rev. Lett. **124**, 025502 (2020).
[29]Y. Tsaturyan, A. Barg, E. S. Polzik, and A. Schliesser, "Ultracoherent nanomechanical resonators via soft clamping and dissipation dilution," Nat. Nanotechnol. **12**, 776–783 (2017).
[30]C. Reetz, R. Fischer, G. G. Assumpcao, D. P. McNally, P. S. Burns, J. C. Sankey, and C. A. Regal, "Analysis of membrane phononic crystals with wide band gaps and low-mass defects," Phys. Rev. Appl. **12**, 044027 (2019).
[31]M. Bückle, Y. S. Klaß, F. B. Nägele, R. Braive, and E. M. Weig, "Universal length dependence of tensile stress in nanomechanical string resonators," Phys. Rev. Appl. **15**, 034063 (2021).
[32]D. Hoch, X. Yao, and M. Poot, "Geometric tuning of stress in predisplaced silicon nitride resonators," Nano Lett. **22**, 4013–4019 (2022).
[33]S. Schmid, K. Jensen, K. Nielsen, and A. Boisen, "Damping mechanisms in high-Q micro and nanomechanical string resonators," Phys. Rev. B **84**, 165307 (2011).
[34]M. H. J. de Jong, M. A. ten Wolde, A. Cupertino, S. Gröblacher, P. G. Steeneken, and R. A. Norte, "Mechanical dissipation by substrate–mode coupling in sin resonators," Appl. Phys. Lett. **121**, 032201 (2022).
[35]D. Shin, A. Cupertino, M. H. de Jong, P. G. Steeneken, M. A. Bessa, and R. A. Norte, "Spiderweb nanomechanical resonators via Bayesian optimization: Inspired by nature and guided by machine learning," Adv. Mater. **34**, 2106248 (2022).
[36]M. J. Bereyhi, A. Arabmoheghi, A. Beccari, S. A. Fedorov, G. Huang, T. J. Kippenberg, and N. J. Engelsen, "Perimeter modes of nanomechanical resonators exhibit quality factors exceeding 10^9 at room temperature," Phys. Rev. X **12**, 021036 (2022).
[37]T. Manzaneque, M. K. Ghatkesar, F. Alijani, M. Xu, R. A. Norte, and P. G. Steeneken, "Resolution limits of resonant sensors with duffing non-linearity," arXiv:2205.11903 (2022).

© Author(s) 2023